Cellular Mechanism of Neuronal Synchronization in Epilepsy

Abstract. *Interictal spikes are a simple kind of epileptic neuronal activity. Field potentials and intracellular recordings observed during interictal spikes of penicillin-treated slices of the hippocampus were reproduced by a mathematical model of a network of 100 hippocampal neurons from the region including CA2 and CA3. The model shows that this form of neuronal synchronization arises because of mutual excitation between neurons, each of which is capable of intrinsic bursting in response to a brief input.*

An interictal spike is an epileptiform brain event that consists, at the cellular level, of the synchronized bursting of a localized population of neurons. Bursting in hippocampal cells consists of rapid sequences of three or more action potentials, possibly interspersed with one or more long-duration action potentials (*1*). In the presence of convulsant agents such as penicillin or bicuculline, interictal spikes occur spontaneously and can be evoked by electrical stimulation, in the neocortex and hippocampus. Interictal spikes occur in vivo (*2*), as well as in vitro in the slice preparation (*3*). Interictal spikes in the slice preparation are similar to those occurring in vivo in their spontaneous periodic occurrence, extracellular field potential, and intracellular bursting, which is correlated with the extracellularly recorded event. Two important questions about interictal spikes concern the mechanism by which synchronization occurs and the reason for the long and variable latency from a stimulus to the onset of an interictal spike.

Experiments were done in the intact transverse hippocampal slice, in the isolated region including CA2 and CA3 (CA2–CA3) and in the isolated CA2 region (*4*). The CA2–CA3 region, which probably contains no more than a few thousand cells, is capable of generating interictal spikes in the presence of penicillin or bicuculline (*3, 5*).

Recent experimental data (*1*) have allowed development of a plausible explanation of bursting in single CA3 neurons (*6*). To investigate synchronization, we have constructed a detailed computer model of 100 CA3 neurons, each capable of intrinsic bursting, interconnected by excitatory chemical synapses. The simulations confirm that the following known phenomena are sufficient to account for synchronized bursting. (i) Each neuron is capable of bursting if sufficiently excited by synaptic input (*1*). (ii) Hippocampal neurons in the CA2–CA3 region are mutually excitatory (*7*). (iii) Recurrent inhibition is blocked by penicillin (*8*). (iv) In spite of such block, bursting can be terminated by an intrinsic cellular inhibitory process, the slow K^+ current. Our model requires that mutual excitation be sufficiently strong that bursting in one cell can evoke bursting in follower cells. Briefly, the mechanism by which an interictal spike arises in our model (*9*) is as follows. When a few cells burst together, either spontaneously or after triggering, they each induce bursting in a few follower cells. These in turn recruit further cells until the majority of the population bursts at once (*10, 11*). Each cell participating will, in general, receive synaptic inputs from other cells, both before and after its intrinsic bursting is triggered—hence the paroxysmal depolarizing shift (*12*). The event is terminated by intrinsic inhibitory processes.

To describe the behavior of single neurons, we used a model (*6*) in which both soma and an apical dendritic region contain active Na^+, K^+, and Ca^{2+} conductances (*13*) and Ca^{2+}-mediated slow K^+ (*14*), so that soma and apical dendrites can burst independently (*1*). The electrotonic structure is shown in Fig. 1A, and a typical burst is shown in Fig. 1B. We let g_K (Hodgkin-Huxley K^+ conductance) have a voltage-dependent inactivation (*15*) while g_{Ca} partially inactivates with increasing intracellular Ca^{2+} (*16*); the detailed mechanism by which individual neurons burst is not critical to the results reported here (*1* .

Because MacVicar and Dudek (*7*) observed excitatory synaptic interactions between CA3 pyramidal cells in 5 of 88 double penetrations, we inferred that each neuron receives input from only a few other cells. Extensive simulations with randomly connected networks of 100 to 400 simplified neurons (*11*) indicated that synchronization could develop if each neuron sent its output to an average of four or more other cells. We constructed a 10 by 10 network (Fig. 1C) by allowing each cell to send synaptic output to any other cell with a probability of .05 (that is, an average of five outputs per cell). Once established, connections remained fixed throughout each simulation. Connections were made to two basal dendritic and two apical dendritic compartments of each connected cell. We did not systematically test the effects of varying the location of the synaptic inputs; the expected effect of such variation would be to vary the latency for spread of bursting from one cell to another. All connections are ex-

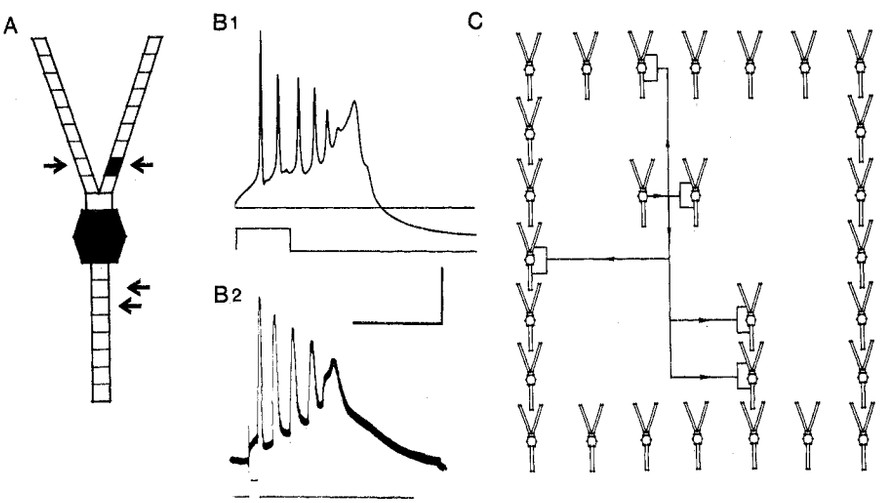

Fig. 1. Structural features of the model. (A) Electrotonic structure of single cell showing division into compartments, soma (central hexagon), basal dendritic cylinder extending below, and branching apical dendrite extending above. Compartments containing active ionic conductances (Na^+, K^+, Ca^{2+}, and Ca^{2+}-mediated slow K^+) are shaded. Locations of excitatory synaptic input are shown by arrows. Each dendritic compartment is 0.1 space constant in electrotonic length. (B1) Intrinsic burst elicited in isolated model neuron by injected depolarizing current (1 nA for 15 msec; lower trace). Calibration: horizontal, 25 msec; vertical, 25 mV, 2.5 nA. (B2) CA3 cell burst evoked by injected current (lower trace). Calibration: horizontal, 40 msec; vertical, 25 mV, 1 nA. (C) Schematic structure of the model neuronal network. For clarity, a 7 by 7 array is shown, although a 10 by 10 array is used in the simulations. Each cell has the structure shown in (A). Every cell sends an output to an average of five other cells, the spatial location of which is random and not related to distance from the original cell. An example of one possible set of outputs for a cell is shown. There are no inhibitory synaptic inputs, and electrotonic junctions do not occur in this model.

0036-8075/82/0514-0745S01.00/0

citatory, since recurrent inhibition is presumed to be blocked by penicillin (*8*). Cells communicate with each other as follows. If the soma membrane potential is greater than 20 mV, its axon is assumed to be active [even if the soma is in a state of depolarization block (*2*)]; the membrane characteristics of axons are not modeled explicitly. A conductance pulse of 0.6 mS/cm^2 is then delivered to all follower cells after a delay of 2.1 msec. This ensures that bursting in one cell will induce bursting in each follower cell, typically after a delay of about 15 msec. The synaptic delay of 2.1 msec is in the observed range (*7*). It is not known if excitatory interneurons occur in this region, so pyramidal cells are assumed to excite one another directly (*18*). Synaptic conductances arising across a cell membrane from two or more other cells add linearly. There were no electrotonic junctions in this model (*19*). Field potentials were estimated by calculating membrane current (I_m) for each compartment of the 100 neurons and summing the I_m terms, each weighted by the reciprocal of the distance squared of the respective compartment from a fixed "recording electrode" (*20*).

When four neighboring cells (called initiating cells) are stimulated with a steady depolarizing current, a cascade of bursting develops, yielding the simulated potentials of Fig. 2A. A similar sequence of events occurs when different sets of cells are stimulated (not shown). The number of cells "bursting" (having fired at least one action potential, but with the soma potential not yet hyperpolarized) rises to 99 and then abruptly falls to 0 (Fig. 2, A1). The simulated field potential (Fig. 2, A2) is "recorded" near the opposite corner from the stimulus. In the simulation, the latency to maximum field potential is 34 msec, which is in the experimental range. Variability of the latency with change in location of the stimulus occurs in this model because, with random interconnections, the precise pattern of spread of bursting depends on the local connectivity. Since, in the model, all cells begin in the resting state, the model does not reproduce the experimentally observed variability of latency for stimuli applied to the same location (*5*); such variability in latency may result from background fluctuations in, for example, bursting threshold. The multiple peaks in the field potential correspond to action potentials in various cells in the network, whereas the positive slow wave corresponds in part to summated slow K^+ currents as well as to synaptic currents. Sample soma membrane potentials are shown in Fig. 2, A3 to A5. Figure 2, A3, shows a double burst in an initiating cell. The first burst was caused by the stimulus, whereas the second was caused by synaptic inputs from other cells bursting during the major part of the interictal spike. Double bursts like this are seen experimentally (Fig. 2, B3). Another (more typical) cell burst is seen in Fig. 2, A4; this long latency burst began 50 msec after onset of the stimulus. All bursts are followed by an afterhyperpolarization. In another simulation, a 1.5-nA hyperpolarizing current was passed through the cell of Fig. 2, A4. This revealed the underlying synaptic event (Fig. 2, A5). This particular cell received synaptic inputs from only two other cells. Cells in the network receiving four or more inputs could not be completely prevented from producing action potentials during interictal spikes when hyperpolarized by as much as 42 mV relative to resting potential (not shown). Experimentally, it was difficult to hyperpolarize most neurons enough to block all action potentials during an interictal spike.

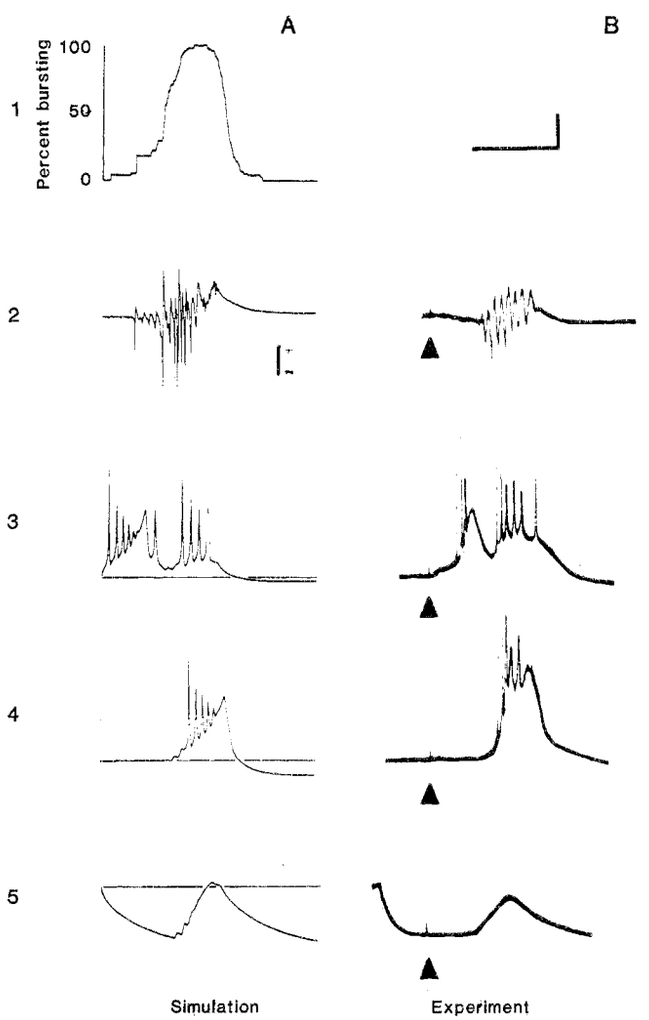

Fig. 2. Simulated and experimentally recorded epileptiform events. (A) Simulated interictal spike, obtained with steady depolarizing current of 1.5 nA to four cells in one corner of network. (A1) Percentage of total cells in network bursting (that is, have fired at least one action potential, but are not yet hyperpolarized). (A2) Field potential. (A3) Simulated soma membrane potential of cell receiving stimulus. Note double burst resulting from EPSP impinging during major part of interictal spike. (A4) Membrane potential of another, more typical, cell. (A5) Membrane potential of same cell as in (A4), with simulation as above, but with 1.5 nA of hyperpolarizing current injected into this cell, revealing underlying EPSP. (B) Experimental interictal spikes, evoked by brief shocks to fimbria and recorded in CA2 region of the pencillin-treated hippocampal slice. (B2) Field potential, isolated CA2. (B3) to (B5) Intracellular records during interictal spikes in intact slice. (B4) and (B5) are from same cell but (B5) is shown during injection of hyperpolarizing current. Triangles mark stimulus artifacts. Calibration: 50 msec in (A) and 60 msec in (B); 25 mV for intracellular records in (A), 4 mV in (B2), and 20 mV in (B3) to (B5).

We propose that epileptiform synchronized bursting is possible because of three experimentally observed features of this system: intrinsic bursting capability, mutual synaptic excitation, and disinhibition. Because of mutual excitation between CA3 cells, the CA2–CA3 region appears to be able to act as a trigger zone for synchronized discharge involving wider regions of the hippocampus (*3*, *5*). CA1, which cannot endogenously generate interictal spikes in the slice (*3*), appears to lack recurrent synaptic excitation (*21*). One specific assumption in our model remains to be verified directly: that bursting in a precursor cell will cause not only an excitatory postsynaptic potential (EPSP), but also bursting in a follower cell. The requirement for disinhibition in our model is not absolute so long as bursting can spread from cell to cell. This model does not elucidate the possible role of electrotonic gap junc-

tions in synchronization (*19*). We have performed additional simulations indicating that dendritic electroresponsiveness, such as we have used, is not required for initiation of interictal spikes if the chemical synapses are sufficiently strong. Whether signal amplification via active dendritic bursting is necessary for synchronization remains to be determined experimentally.

ROGER D. TRAUB
IBM Watson Research Center, Yorktown Heights, New York 10598, and Neurological Institute, New York 10032

ROBERT K. S. WONG
Department of Physiology and Biophysics, University of Texas Medical Branch, Galveston 77550

References and Notes

1. R. K. S. Wong and D. A. Prince, *J. Neurophysiol.* **45**, 86 (1981); ———, A. I. Basbaum, *Proc. Natl. Acad. Sci. U.S.A.* **76**, 986 (1979).
2. M. Dichter and W. A. Spencer, *J. Neurophysiol.* **32**, 649 (1969); *ibid.*, p. 663.
3. P. A. Schwartzkroin and D. A. Prince, *Ann. Neurol.* **1**, 463 (1977); *Brain Res.* **147**, 117 (1978).
4. Guinea pig transverse hippocampal slices were prepared and perfused as described (*5*). Sodium penicillin (1.7 m*M*) was included in the bathing medium. Interictal spikes, with corresponding multipeaked field potentials and simultaneous intracellular bursting, were recorded in CA2–CA3; these events occurred either spontaneously or were elicited by local stimuli. The isolated CA2–CA3 region was obtained by making a cut across the transverse slice extending from the superior alveus to the inferior alveus. The cut began at a point on the superior alveus about 1.4 mm from the fornix and ended on the inferior alveus about 1 mm from the fornix. The cut separated the CA1 cells, the granule cells, and some of the CA4 cells from the CA2–CA3 region. CA2 was isolated by making an additional cut from the alveus to the hippocampal fissure. This cut began at a point on the superior alveus about 0.7 mm from the fornix.
5. R. K. S. Wong and R. D. Traub, *J. Neurophysiol.*, in press.
6. R. D. Traub, *Neuroscience*, in press.
7. B. A. MacVicar and F. E. Dudek, *Brain Res.* **184**, 220 (1980).
8. R. K. S. Wong and D. A. Prince, *Science* **204**, 1228 (1979); R. Dingledine and L. Gjerstad, *Brain Res.* **168**, 205 (1979).
9. This model applies most directly to stimulus-evoked interictal spikes wherein the stimulus itself serves to synchronize a small group of cells. Presumably, the initial event in a spontaneous interictal spike is also the synchronous discharge of a small group of cells. The mechanism by which this initial synchronization comes about during a spontaneous interictal spike is not considered here.
10. R. D. Traub and R. K. S. Wong, *Neuroscience* **6**, 223 (1981).
11. ———, *J. Neurophysiol.*, in press.
12. E. S. Goldensohn and D. P. Purpura, *Science* **139**, 840 (1963); D. A. Prince, *Exp. Neurol.* **21**, 467 (1968); D. Johnston and T. H. Brown, *Science* **211**, 294 (1981).
13. P. A. Schwartzkroin and M. Slawsky, *Brain Res.* **135**, 157 (1977); R. K. S. Wong and D. A. Prince, *Brain Res.* **159**, 385 (1978).
14. B. E. Alger and R. A. Nicoll, *Science* **210**, 1122 (1980); J. R. Hotson and D. A. Prince, *J. Neurophysiol.* **43**, 409 (1980).
15. R. W. Aldrich, Jr., P. A. Getting, S. H. Thompson, *J. Physiol. (London)* **291**, 507 (1979).
16. D. Tillotson, *Proc. Natl. Acad. Sci. U.S.A.* **76**, 1497 (1979).
17. Parameters of this model include: R_{input} = 32 megohms; R_m = 10,000 ohm-cm^2, C_m = 3 μF/cm^2, τ_m = 30 msec, $\bar{g}_{Na}$ = 75 mS/cm^2, and the R_{input} of active dendritic branch is 90 megohms, where R_{input} is input resistance, R_m is membrane resistivity, C_m is membrane capacitance, τ_m is a membrane time constant, and $\bar{g}_{Na}$ is maximum sodium conductance. Time constants for removal of g_{Ca} inactivation and for decrease of slow K^+ conductance were different for each cell, varying from 182 to 222 msec and 446 to 571 msec, respectively. For other parameters, see (*6*). Differential equations modeling each neuron were integrated by using a second-order Taylor series with time step dt = 50 μsec. The membrane potential is not altered when dt = 33 μsec. The equations were embodied in a set of PL/I programs and run on an IBM 370 model 168 computer. A simulation of 120 msec of activity used 14.4 minutes of CPU time.
18. Synchronization in the model occurs over a range of synaptic strengths, so long as bursting can spread from cell to cell. The exact value of synaptic strength determines the time it takes for spread of bursting and hence determines the sharpness of synchronization (R. D. Traub and R. K. S. Wong, in preparation). It is reasonable to assume that bursting in one cell can indeed evoke bursting in another: a 2-msec injected current depolarizing a CA3 cell 2 to 5 mV can evoke a burst (*1*). Recurrent EPSP's larger than this have been reported (*7*), although direct comparison is difficult since in this case the postsynaptic neuron was hyperpolarized. Previous work [T. H. Brown, R. K. S. Wong, D. A. Prince, *Brain Res.* **177**, 194 (1979)] has shown that spontaneous EPSP's can depolarize CA3 cells up to 4 mV. Multiple burst initiation sites in soma and dendrites (*1*) may contribute to the spread of bursting.
19. B. A. MacVicar and F. E. Dudek, *Science* **213**, 782 (1981).
20. This model is distinguished from our earlier one (*10*) in a fundamental way; in the present model, each neuron connects only to a few other cells, rather than to 60 or more as in the earlier study. In addition, each neuron is now represented more realistically. Although the previous study showed the importance of recurrent excitation, the anatomical assumptions were less accurate than in the present model, and it was unable to reproduce field potentials of long latency.
21. W. D. Knowles and P. A. Schwartzkroin, *J. Neurosci.* **1**, 318 (1981).
22. We thank F. A. Dodge, Jr., and G. J. Lasher for reviewing the manuscript. Supported in part by NIH grant NS18464 and a Klingenstein fellowship award (to R.K.S.W.).

7 January 1982; revised 19 March 1982

New Dopaminergic and Indoleamine-Accumulating Cells in the Growth Zone of Goldfish Retinas After Neurotoxic Destruction

Abstract. *Juvenile goldfish were allowed to grow for 3 months after dopaminergic or indoleamine-accumulating cells in their retinas had been destroyed by intravitreal injection of 6-hydroxydopamine or 5,7-dihydroxytryptamine, respectively. New cells of each type were found growing in concentric rings at the margin of the retina. To compensate for the loss of dopaminergic innervation in retinas treated with 6-hydroxydopamine, cells in the growth zone appeared to proliferate at a higher rate than those in untreated retinas and long processes were extended into the retina by the first dopaminergic cells to appear.*

In histological and histochemical studies of retinal enlargement in the goldfish eye, Easter and his colleagues (*1*) found that the number of neurons per retina increases with growth while the density (except for rods) decreases (*1*, *2*). Thymidine autoradiography has demonstrated that cell proliferation leading to the formation of new neurons takes place only in the peripheral zone neighboring the ora terminalis (*2*). Therefore, new retinal tissue is added in concentric rings. Fluorescence microscopic studies of goldfish and carp retinas have revealed that, with increasing diameter of the retina, dopaminergic (DA) cells (*3*) and indoleamine-accumulating (IA) cells (*4*) also increase in number while decreasing in density (*5*). This pattern of growth is thus identical to that described for other classes of retinal cells (*2*).

In the retinas of adult carp (body length, 30 to 35 cm), DA cells are destroyed by intravitreal injection of 6-hydroxydopamine (6-OHDA), and IA cells are destroyed by 5,7-dihydroxytryptamine (5,7-DHT) (*6*). Total destruction of IA cells can be achieved by a

Table 1. Body length, eyeball diameter, retinal growth zone width, and DA and IA cell density in control goldfish and in goldfish treated with 6-OHDA or 5,7-DHT 3 months before eyeball enucleation. Growth zone width and cell density are corrected for tissue shrinkage in the fixative (*5*). Values are means ± standard errors.

Group	Body length, tip to tip (cm)	*N**	Eyeball diameter, horizontal (mm)	Growth zone width (μm)	Cells per square millimeter	
					DA	IA
6-OHDA–treated	12.0 ± 0.5	7	7.0 ± 0.1	252 ± 37	186.4 ± 54.0†	200.6 ± 53.0†
5,7-DHT–treated	12.5 ± 0.7	5	7.0 ± 0.1	251 ± 42	144.3 ± 51.9	166.6 ± 41.2
Control, end of experiment	12.3 ± 0.8	6	7.1 ± 0.1	252‡	112.6 ± 16.7	132.2 ± 13.2

*Number of retinas examined. †Significantly different from corresponding control value at $P < .02$ (Student's *t*-test). ‡Corresponds to the mean value for growth zone width in all the treated retinas.

0036-8075/82/0514-0747$01.00/0